Journal of Neuroscience Methods 255 (2015) 29–37

Contents lists available at ScienceDirect

Journal of Neuroscience Methods

journal homepage: www.elsevier.com/locate/jneumeth

Basic neuroscience

A multi-site array for combined local electrochemistry and electrophysiology in the non-human primate brain

Anita A. Disney[a,*,1], Collin McKinney[c], Larry Grissom[b], Xuekun Lu[b], John H. Reynolds[a]

[a] Systems Neurobiology Laboratories, The Salk Institute for Biological Studies, La Jolla, CA, USA
[b] California Institute for Telecommunications and Information Technology (CalIT2), University of California San Diego, La Jolla, CA, USA
[c] Department of Chemistry, University of North Carolina at Chapel Hill, Chapel Hill, NC, USA

HIGHLIGHTS

- We present a novel multi-contact recording array and supporting headstage.
- The system allows concurrent *in vivo* electrochemistry and electrophysiology.
- The system is validated using measures of arousal in an awake macaque monkey.
- A detailed protocol for device fabrication by photolithography is provided.

ARTICLE INFO

Article history:
Received 9 July 2015
Accepted 13 July 2015
Available online 29 July 2015

Keywords:
Amperometry
Neuromodulation
Primate
Cortex
Visual system

ABSTRACT

Background: Currently, the primary technique employed in circuit-level study of the brain is electrophysiology, recording local field or action potentials (LFPs or APs). However most communication between neurons is chemical and the relationship between electrical activity within neurons and chemical signaling between them is not well understood *in vivo*, particularly for molecules that signal at least in part by non-synaptic transmission.
New method: We describe a multi-contact array and accompanying head stage circuit that together enable concurrent electrophysiological and electrochemical recording. The array is small (<200 μm) and can be assembled into a device of arbitrary length. It is therefore well-suited for use in all major *in vivo* model systems in neuroscience, including non-human primates where the large brain and need for daily insertion and removal of recording devices places particularly strict demands on design.
Results: We present a protocol for array fabrication. We then show that a device built in the manner described can record LFPs and perform enzyme-based amperometric detection of choline in the awake macaque monkey.
Comparison with existing methods Existing methods allow single mode (electrophysiology or electrochemistry) recording. This system is designed for concurrent, dual-mode recording. It is also the only system designed explicitly to meet the challenges of recording in non-human primates.
Conclusions: Our system offers the possibility for conducting *in vivo* studies in a range of species that examine the relationship between the electrical activity of neurons and their chemical environment, with exquisite spatial and temporal precision.

1. Introduction

The ability to concurrently measure the electrical activity of neurons (action potentials and/or local field potential) and non-synaptic neuromodulatory signals, both on fast timescales, will be central to understanding cortical circuits. Excellent connectivity maps exist for many neural circuits, and in the case of some organisms, such as *Caenorhabditis elegans* we have the full neural circuit diagram. In several organisms, we also have excellent descriptions of the firing responses of individual neurons within those circuits to diverse sensory inputs, and in many cases the patterns or correlated firing across large populations of neurons. In some animal models, we have characterized the responses of neurons during complex cognitive tasks involving selective attention, reward prediction, and quantity estimation. And yet we continue to struggle to

* Corresponding author. Tel.: +1 615 322 6090; fax: +1 615 343 8449.
E-mail address: anita.disney@vanderbilt.edu (A.A. Disney).
[1] Current address: Department of Psychology, Vanderbilt University, Nashville, TN, USA.

http://dx.doi.org/10.1016/j.jneumeth.2015.07.009

explain or predict behavior from circuit structure or from momentary neural activity. In part this is because missing from the above descriptions is an understanding of connectivity that is not made *via* synapses, and of signals that modulate rather than generate action potentials. That is, the neuromodulators are largely absent from our current descriptions of the nervous system. This absence is particularly notable in descriptions of the cortical circuits of large mammals, including primates.

Neuromodulators signal key variables related to context and internal state (reviewed by Dayan, 2012; Marder, 2012) and in doing so they profoundly alter the activity of the circuits within which they act. Many neuromodulators operate, at least in part, by non-synaptic means—a signaling mode often referred to as volume transmission (Vizi et al., 2004). In order to understand the interplay between volume transmitted neuromodulators and the activity of the cortical circuits into which they are released we need a means to record both the concentration of various signaling molecules in the extracellular space, and the activity of the nearby neurons. We need to be able to make these recordings in a spatially precise fashion, on timescales relevant to behavior, and in various model systems.

Electrophysiological recording techniques are well developed in neuroscience, and the field of electrochemistry has made exciting inroads into the field in recent years (Burmeister et al., 2000; Parikh et al., 2007, 2004; Park et al., 2011). Concurrent intracranial electrochemical and electrophysiological recording has been possible with separate sensors since the early 1980s (Bickford-Wimer et al., 1991; Hefti and Felix, 1983). However, with the notable exceptions of switched circuits for the measurement of local catecholamine concentration and local electrophysiological activity (Stamford et al., 1993; Takmakov et al., 2011) and a system limited to measurement of low frequency local field potentials (Zhang et al., 2009) electrochemistry and electrophysiology – each of which offers exquisite spatial and temporal precision – have not yet been combined into a single sensor in service of fully concurrent recording of a wide array of extracellular molecules with diverse measures of electrical activity of neurons. In addition to this gap in our capabilities, it is also the case that the excellent electrochemical recording devices that have been designed to detect molecules other than catecholamines (Burmeister et al., 2000) are too large (and therefore destructive of tissue) for use in daily recording in non-human primates.

Here we describe a four channel multi-electrode array that modifies the capabilities of an existing multi-channel electrochemical device (Burmeister et al., 2000), combines those capabilities with the ability to record isolated action potentials and/or full spectrum local field potentials, and reduces the device diameter approximately fivefold. We also describe supporting hardware that modifies the capabilities of an existing switched recording mode (Takmakov et al., 2011) to enable concurrent electrochemical and electrophysiological detection. The result is a device that can be used to make repeated measurements of interesting non-synaptic signaling molecules and local neural activity, over time in the awake and behaving non-human primate. We validate this recording device using non-concurrent *in vivo* measurement of extracellular choline concentration (as a reporter for the activity of the cholinergic system) and local field potentials (as a measure of neural activity) in an animal moving naturally between various states of arousal.

2. Materials and methods

2.1. Array fabrication and assembly

The multi-site arrays are made in a two-step process. In the first step (described in Section 2.1.1) ceramic wafers are patterned with recording sites and insulation and are diced into individual "tips". These tips are then wire bonded, assembled into hypodermic tubing and soldered onto connectors (described in Section 2.1.2).

The recording device tips have four contact sites (Fig. 1A). Two sites are 300×15 μm and are designed for electrochemical recording in parallel single-channel or referenced (subtractive or 'sentinel' mode: Burmeister et al., 2000). The other two sites are 15×15 μm and are used for electrophysiological recording. Connecting lines run from these contacts to the distal end of the device tip and terminate in 200×75 μm bonding pads. Patterned scribe lines guide the dicing of ceramic wafers into individual tips.

2.1.1. Two-layer photolithograpy and dicing

One inch square Superstrate 996 polished alumina ceramic wafers (Coorstek, Inc, Golden, CO, USA) are cleaned (10 min with ultrasonic agitation in each of the following: acetone, methanol, isopropanol, and de-ionized water) and dried with a nitrogen gun before spin coating with a ~1.3 μm layer of S1813 photoresist (Shipley Microposit, Marlborough, MA, USA).

After a 1 min pre-bake at 115 °C, the wafers are exposed for 4 s at 11 mW/cm^2 using an MA-6 mask aligner (Karl Suss). The first layer mask (Fig. 1B, top left) was developed using the Layout Editor software package (Juspertor, Germany). The pattern is printed as a dark field mask at 40,000 DPI resolution on Mylar (Fineline Imaging, Colorado Springs, CO, USA). The resulting transparency is taped onto a soda lime glass carrier (Fineline Imaging) for use in the mask aligner.

After developing the photoresist (with Shipley MF319 developer) and conducting a visual examination under 10× magnification to confirm good patterning, the wafers are briefly de-scummed (1 min under oxygen at 200 mT pressure, 200 W power: Technics PE-11B etcher) before metal deposition. Metals are deposited using an AJA ATC Orion DC sputtering system. First, a 5 nm titanium adhesion layer is applied using a gun power of 200 W, under Argon gas at 5 sccm, 3 mT. This is followed by deposition of 250 nm of platinum with a gun power of 300 W, under Argon gas at 5 sccm, 3 mT. Lift-off of the excess metals is achieved in acetone under ultrasonic agitation, after which the wafers are re-cleaned (in acetone, methanol, isopropanol, and water as described above) and dried using a nitrogen gun.

The second layer photoresist is SU-8; a biocompatible insulator. SU-8 2001 (MicroChem Corp, Westborough, MA, USA) is spin-coated over the deposited metals and pre-baked for 2 min at 95 °C. This layer is then exposed for 3.2 s at 11 mW/cm^2 using an MA-6 aligner. The second layer mask (Fig. 1B, bottom right) is a clear field mask printed at 40,000 DPI resolution on Mylar and then taped to a soda line glass carrier.

After exposure, the SU-8 is post-baked on a hotplate for 3 min at 95 °C and then developed (using SU-8 developer, MicroChem) for 60 s with ultrasonic agitation. If visual inspection indicates that the openings in the insulation over the contact sites are too small (or not fully open), the SU-8 is developed further. Once a good result has been achieved (determined by eye using a 10× or 20× objective), the wafer is rinsed in isopropyl alcohol and dried before a final descum (Technics PE-11B etcher; 3 min under oxygen at 200 mT, 200 W).

The wafers are then mounted onto UV-release tape and diced into individual tips with a DISCO DAD 3220 Automated Dicing Saw using a 20 μm electroformed blade running at a speed of 0.2 mm/s. The diced wafers are released by UV exposure and stored in low adhesion (XT) gel-pak carriers (Gel-Pak, Hayward, CA, USA) ready for wire bonding.

2.1.2. Wire-bonding

To each bonding pad on each device tip, a 10 cm length of 99.9% pure 0.002 in. platinum wire with 1× polyimide insulation

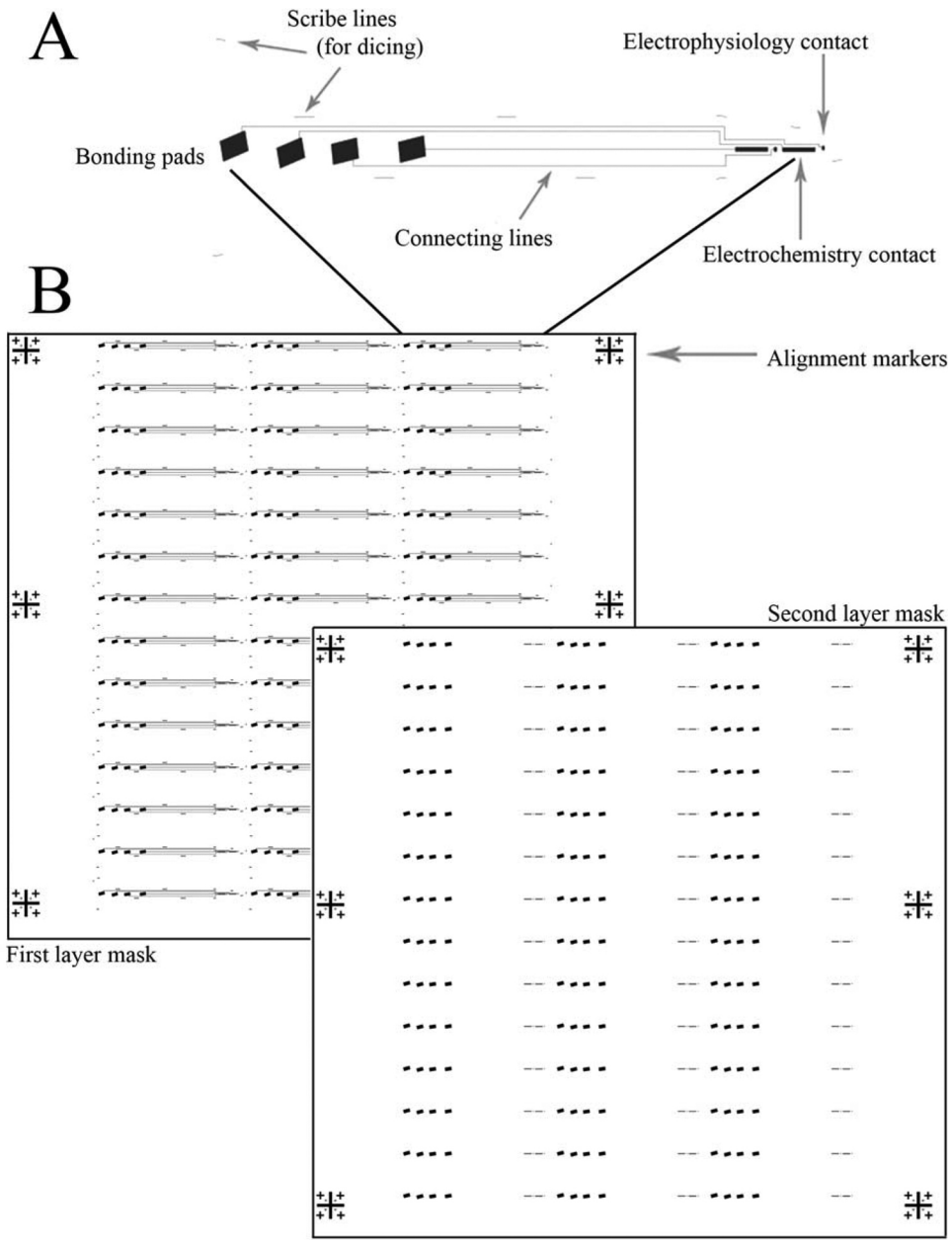

Fig. 1. Recording tip circuit and photolithographic masks. Panel (A) shows the detail of one recording tip, each tip has four platinum contact sites. The two electrochemistry contacts are 300 × 15 μm and the two electrophysiology contacts are 15 × 15 μm. The connecting lines are 10 μm wide and run from the recording contacts to the distal end of the device tip, terminating in four 200 × 75 μm bonding pads. Patterned scribe lines guide the dicing of ceramic wafers into individual tips. Multiple tips are patterned onto a single ceramic wafer using the first layer mask ((B) top left). This pattern (without the arrows and text) is printed at 40,000 DPI resolution as a *dark field* mask on Mylar. The field shown is for use with a 1 × 1 in. wafer. Forty-two device tips are patterned onto each wafer. Three sets of alignment markers on each side of the primary pattern facilitate alignment with the second layer pattern. The resulting transparency is taped onto a clean soda lime glass carrier for use in the mask aligner. The insulation layer is patterned using the second layer mask ((B) bottom right). As with the first layer, this pattern is printed at 40,000 DPI resolution on Mylar. The second layer is, however, a *clear field* mask. The field shown is for use with a 1 × 1 in. wafer and the alignment markers on each side of the primary pattern ensure alignment with the corresponding first layer pattern. The only features that appear on the pattern are the recording contacts and bonding pads, where openings in the insulation are needed. The transparency is taped onto a clean soda lime glass carrier for use in the mask aligner.

(California Fine Wire, Grover Beach, CA, USA) is attached by ultrasonic wedge bonding. To stabilize tips for bonding, they are glued to a 1 × 1 in. quartz glass slide (Electron Microscopy Services) using super glue gel (Gorilla) and allowed to dry.

The bonding is done using a West: Bond 7476E wedge bonder reconfigured for 5 W output (usual is 2.5 W). The spring is removed from the tool carrier so that the force applied is the dead weight of the bonding tool (∼380 g). The bonding tool is matched to the bonding pad size (here 200 × 75 μm), wire diameter (here 0.002 in), and thickness of polyimide insulation (here 1×, effectively 0.0007 in.). The tool specifications (both purchased from DeWeyl Tools) we have used successfully are:

(a) MF-108-1/16-750-.006-.007-M-N-2.4 TDF = 0.040, GD0.001, or
(b) MF-108-1/16-750-.008-.008-M-N-2, TDF = 0.040, GD0.0008.

The insulated wire is positioned by hand over the bonding pad and bonded using the following settings:

Power: 850 (arbitrary units: effective range 750–900); time: 275 ms (effective range 225–300); stage temperature: 100 °C; tool temperature: 100 °C.

The device tip with bonded wires is then removed from the quartz glass carrier by careful immersion in an acetone bath, gently cleaned through methanol, isopropanol, and water and stored individually in gel-pak carriers.

2.1.3. Device assembly

Thin-walled, 304 grade stainless-steel hypodermic tubing is used to insert the tips into the brain. The tubing is cut by hand using a rotary tool (Dremel) to a length appropriate for the depth of the target structure (and height of recording cylinder, if used). Different gauges should be tested for their ability to accommodate the diameter of the device plus bonded wires. The *in vivo* recordings described here were made using devices assembled into 27-ga tubing (nominal outer diameter 400 μm, McMaster–Carr). Assembly has been successful into tubing down to 30 ga (300 μm nominal OD). Using a Dremel fitted with a 0.025 in. disc cutting tool, one end of the tubing is beveled to assist with insertion and alignment of the tip (Fig. 2A). The tubing must be carefully deburred at both cut ends with fine grit sandpaper before continuing.

The distal end of the bonded platinum wires (with respect to the device tip) are inserted into the beveled end of the tubing and passed through the tubing lumen until the tip is at the level of the beveled shelf. The tip is then aligned such that it extends beyond the end of the shelf as desired (Fig. 2B) and a very small amount of super glue liquid (Loctite) is applied over the wire bonds. The glue is allowed to wick underneath the ceramic tip and the excess removed. A full 24 h curing time is allowed before continuing with assembly.

Once the super glue has cured, a one cm length of platinum wire at the distal end is stripped of polyimide using a small volume (~15–20 mL) of 37 N sulfuric acid heated to 60–80 °C. A 1-min exposure to the acid is normally sufficient. The wires are dipped in de-ionized water and inspected under a microscope. If insulation remains, the acid strip is repeated as needed. For reasons of safety this step must be performed in a fume hood.

The stripped ends of the wire are then soldered to the desired connector (determined by the supporting electrochemistry and electrophysiology hardware) and stabilized with epoxy. This device requires a sharpened guide tube or artificial dura in large mammals (such as the macaque monkey).

2.2. In vivo *recording*

2.2.1. Animal model

Test recordings were made in an adult male rhesus macaque (*Macaca mulatta*) monkey. All procedures were approved by the Institutional Animal Care and Use Committee (IACUC) at the Salk Institute. The animal had been trained to sit in a primate chair and had a recording cylinder implanted over the primary visual cortex as part of unrelated physiology experiments.

2.2.2. Enzyme coating

Prior to use, the fully-assembled recording device is cleaned, sterilized (10 min each in 100% filtered isopropyl alcohol; then 70% filtered isopropyl alcohol; and finally sterile, de-ionized water), and allowed to air dry. Once dry, three coats (approximately 0.35 μL each) of choline oxidase (Sigma, cat C4405) solution are applied to one of the electrochemistry contacts (choline oxidase solution: 0.2 units/μL choline oxidase, 0.9% bovine serum albumin, 0.11% glutaraldehyde in water). To the other electrochemistry contact, the same volume of 0.9% bovine serum albumin, 0.11% glutaraldehyde in water is applied (*i.e.* the carrier solution, but not the enzyme). These coatings are allowed to cure for 24–48 h prior to use.

2.2.3. Exclusion layer coating

An electropolymerized layer of meta-phenylenediamine (mPD) excludes interferents from the recording sites. Nitrogen is bubbled through sterile 0.05 M phosphate-buffered 0.9% saline (PBS) for a minimum of 25 min to displace dissolved oxygen and then this PBS is used to make a 5 mM mPD solution. The solution is electropolymerized onto the two electrochemistry recording sites (not the electrophysiology sites) using cyclic voltammetry between +0.2 and +0.7 V *versus* Ag/AgCl at a scan rate of 50 mV/s for 20 min.

2.2.4. In vitro *calibration*

After soaking in sterile 0.05 M PBS for 1 h, electrodes are calibrated in stirred sterile 0.05 M PBS at 37 °C by constant potential amperometry (−0.7 V) *versus* Ag/AgCl reference using the FAST16 MKII potentiostat (Quanteon, Lexington, KY). The change in current is measured across sequential additions of test solutions that yield the following in-bath concentrations: 250 μM ascorbic acid (interferent); three additions of 20 μM choline chloride; and 2 μM dopamine. Selectivity and limits of detection are calculated for both channels.

Prior to recording the impedance of the electrophysiology contacts is measured at 1 kHz in 0.9% sterile saline.

2.2.5. Recording in the macaque

Movement through various states of arousal was used as the positive *in vivo* control. A sintered AgCl reference electrode (Warner Instruments) was sterilized in 70% isopropyl alcohol for 10 min and then soaked in sterile 0.05 M PBS overnight prior to recording. A sterile custom sharpened guide tube and the recording device were loaded onto a micropositioner and the positioner attached to the animal's recording chamber. After the guide tube had passed through the dura, the recording device was advanced into the tissue. Once at the desired depth, the recording cylinder was filled with sterile .05 M PBS and the reference electrode placed inside the cylinder. Electrochemical recordings were made with respect to this Ag/Cl reference. Electrophysiological recordings used the guide tube as a reference. Only one system (electrochemistry or electrophysiology) was connected at a time to avoid ground loops. See Section 2.4 for details of a system that allows concurrent recording.

Driving a recording device into the brain compresses the tissue to some degree. After a period of 10–15 min to allow the brain tissue to "catch up" with the device insertion, electrochemical recordings began. The FAST 16 system was connected *via* a 2 pA/μV headstage to the pins carrying output from the two electrochemical contacts. A further period of 15 min, with a constant potential of −0.7 V *versus* AgCl applied, allowed for the non-Faradaic current to relax out, leaving a stable baseline for recording. The signal was sampled at 40 Hz and stored for offline analysis. The animal was seated in a dimly lit room and allowed to move naturally through various states of arousal. Arousal was assessed by behavioral measures (eye opening and closing) recorded using an infra-red video camera focused on one eye (ISCAN). Wakefulness was defined as a period of no less than 2 min with the eyes fully open. Drowsiness was defined as a period of no less than 2 min with the eyes fully closed. Data were analyzed for the 2 min after the criterion time period has been reached. So for an "eyes open" data point to be recorded, the eyes had to be open for no less than 4 min, two to reach criterion and then at least further 2 min for data collection. Eye position data (analog signal) and manual TTL pulses indicating the start of an "awake" or "drowsy" period (delivered *via* the FAST16 interface) were passed to a Plexon system (see below) to enable co-registration of the data. When collecting electrochemical data, only the eye position and TTLs were being received by the Plexon software.

Once electrochemical recordings were complete, the FAST16 system was completely disconnected from the electrode and a Multichannel Acquisition Processor (Plexon) connected to the

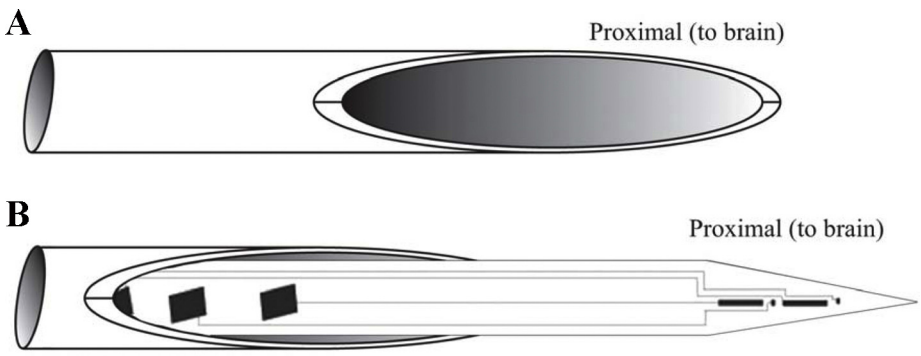

Fig. 2. Assembly of recording tip into carrier tubing. Schematic is not to scale and is intended to illustrate the shaping of the tubing and the relative positioning of the ceramic within it. The device dimensions vary according to fabrication decisions. Our mask and dicing parameters result in a tip width up to 200 μm which can easily be assembled into tubing down to 30 ga (300 μm outer diameter). (A) Beveled end of hypodermic tubing. The hypodermic tubing can be seen as having a proximal end (were the recording tip will emerge) and a distal end (where the wires will emerge and be soldered onto a connector). Proximal and distal in this case are defined in relation to the tissue during recording. The proximal end is beveled with a hand held rotary tool. This beveled end facilitates alignment of the ceramic recording tip with the tubing. (B) Positioning of the recording tip during assembly. The recording tip is fed backwards into the tubing, wires first (wires not shown) until just the desired length is protruding. Positioning the bonding pads within the lumen of the tubing protects the delicate wire bonds they carry, as does the super glue used to anchor the recording tip to the carrier tube. The recording contacts should be beyond the proximal tip of the beveled tubing, to ensure good contact with the tissue.

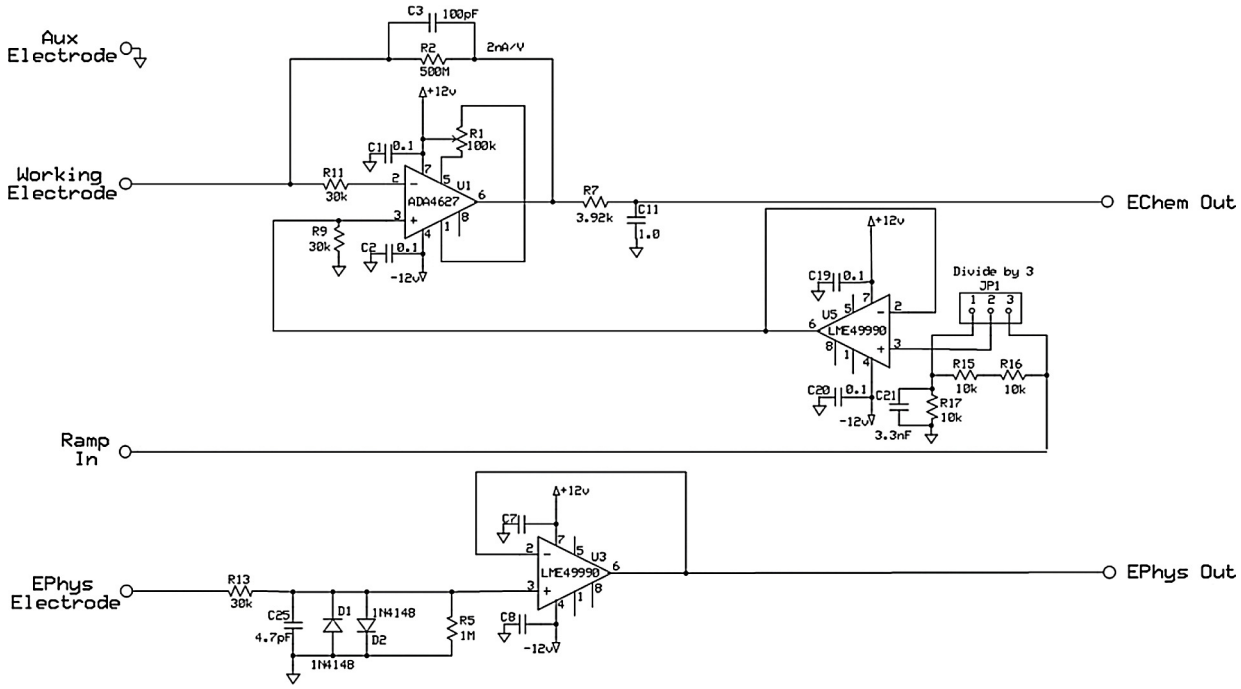

Fig. 3. Circuit schematic for dual mode headamp. Only one electrophysiology and one electrochemistry channel is shown. The electrodes are on the left: aux electrode is the Ag/Cl reference and also serves as gound. The working electrode provides electrochemical recordings and has circuitry to provide the needed voltage ramps/holding potentials. The ephys (electrophysiology) electrode provides electrophysiological recordings. This headamp is connected to a potentiostat *via* a DB 25 connector (not shown).

two channels carrying output from the electrophysiology contacts. Local field potential (LFP) recordings allow spectral analysis and identification of drowsy and wakeful periods. To extract the LFP, the signals were amplified (×1000), bandpass filtered (0.7 Hz to 170 Hz), and digitized at 1 kHz. The video recording of eye opening/closing was continuous throughout the electrochemical and electrophysiological recordings. Eye position was also passed directly as an analog input to the Plexon system and saved in the same file as the physiological recordings. The start of "awake" or "drowsy" periods, as defined above, were marked by manual TTL pulses.

Once recording was complete, the recording device, guide tube and AgCl reference were retracted, and the recording cylinder cleaned and sealed.

2.3. Data analysis

2.3.1. Electrochemistry

Data was exported from the FAST software (Quanteon) as a .csv file and then imported into Matlab (Mathworks) for analysis. The first 15 min of data were discarded (to exclude the highly non-stationary portion at the start of the recording). The next 5 min of data were treated as the "baseline" for the rest of the recording. The animal did not fall asleep during this first 20 min of recording due to activities of the experimenter in the recording room. During the subsequent 60 min there were two "awake" periods and two "asleep" periods (during the rest of the recording the animal's eyes did not remain fully open or fully closed for the requisite 4 min total for analysis).

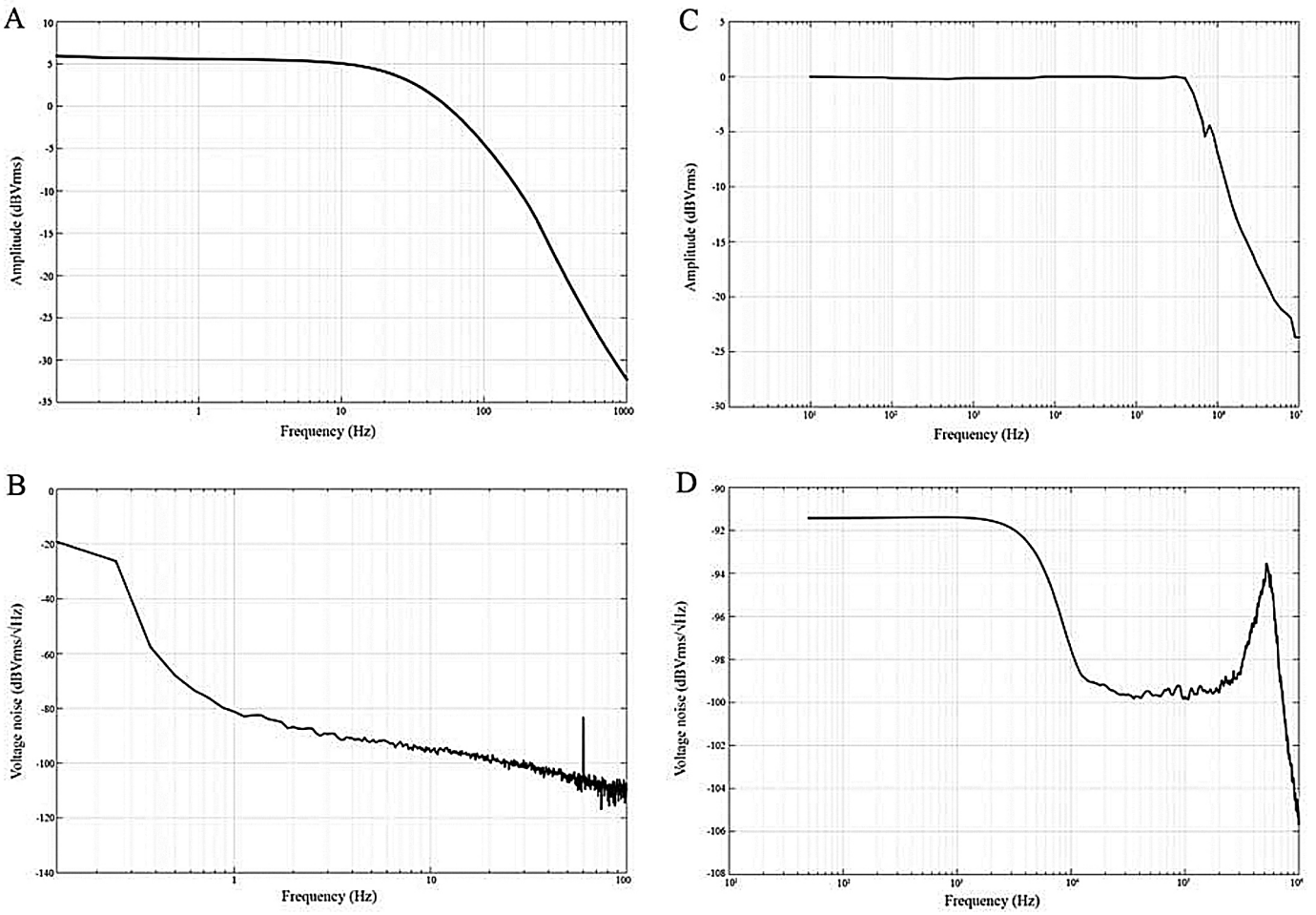

Fig. 4. Amplifier and voltage follower response profiles. (A) Transconductance amplifier frequency response. Frequency response plot for the transconductance amplified with a 10 MΩ "dummy" resistor in place of the electrodes. (B) Transconductance amplifier spectral noise density. Plot of spectral noise density *versus* frequency for the transconductance amplifier with a 10 MΩ "dummy" resistor in place of the electrodes. The data in this plot was integrated and converted to a current using Eq. (1) to obtain the total noise measurement of 85 pA_{rms} (10 mHz–100 Hz). The small spike on the right hand corner is residual 60 Hz line noise. (C) Voltage follower frequency response. Frequency response plot for the voltage follower amplifier with the input shorted. (D) Voltage follower noise spectral density. Plot of spectral noise density *versus* frequency for the voltage-follower amplifier with the input shorted. Noise gain effects result in the noise peak near the amplifier −3 dB point (see text).

Table 1
Impedance characteristics of 15 × 15 μm Pt contacts for electrophysiological recording.

Mean (±SD)	Mode	Minimum	Maximum
0.5 MΩ (±0.4)	0.5 MΩ	0.05 MΩ	1.5 MΩ

There were two channels of electrochemical data, one from the contact with an enzyme coating (the "choline" channel) and one from the contact coating with the carrier solution only (BSA + glutaraldehyde; the "sentinel" channel). To correct for current resulting from endogenous interferents, the measured sentinel channel currents were subtracted, point-by-point, from the measured choline channel currents.

Using the TTL pulses recorded on the data file, the average current for the 2 min period following each eye opening and eye closing was calculated.

2.3.2. Electrophysiology

All analyses of local field potentials (LFP) were performed using a combination of custom Matlab code and the Chronux Matlab Toolbox (http://chronux.org). Fifty-one minutes of data were analyzed and reported during which there was a single eyes-closed (*i.e.* "asleep") period of greater than 4 min and a prolonged (23 min duration) eyes-open ("awake") period. Five, 2-s segments of the LFP data, each separated by 20 s, were taken from the start of these two periods (one eyes-open period, one eyes-closed period) and the average power spectrum calculated.

2.4. Headamp for concurrent recording

A specialized headamp has been designed to allow simultaneous, multi-channel chronoamperometry and electrophysiological measurements. This headamp consists of two channels of transconductance amplifiers for performing chronoamperometry and two channels of voltage-follower amplifiers used for performing the electrophysiological measurements. This schematic for this circuitry can be seen in Fig. 3. The transconductance amplifiers are similar to those described in (Takmakov et al., 2011) except that the gain is much higher and the bandwidth has been limited. The applied potential is buffered by a voltage-follower prior to being presented to the non-inverting input of the transconductance amplifier. Since many experiments are performed with applied potentials between ±3 V, a 1:3 attenuator can be selected in order to utilize the full bit depth resolution of a ±10 V DAC (digital-to-analog converter) for greatest accuracy. By applying the potential to the non-inverting input and by connecting the Working Electrode (WE) to the inverting input, the WE is held at the desired

Table 2
Electrochemical recording properties before and after device use *in vivo*. LOD—limit of detection; selectivity—choline:AA ratio.

	Mean LOD before recording ($n = 5$)	Mean selectivity before recording ($n = 5$)	Mean LOD after recording ($n = 3$)	Mean selectivity after recording ($n = 3$)
Choline channel	0.8 μM (range: 0.04–2)	37:1 (range: 7–81)	12.5 μM (range: 6–16)	7:1 (range: 1–18)
Sentinel channel	191 μM	10:1	314 μM	2:1

potential while the current flowing between the WE and ground is measured. A jumper allows both channels to track the same applied potential or for each channel to operate independently. The gain of the transconductance amplifier is

$$\text{Gain} = \frac{-I_{\text{in}} \times R_f}{V_{\text{out}}} = \frac{2nA}{V} \quad (1)$$

where I_{in} is the measured current; R_f is the feedback resistor (500 MΩ).

The output of the transconductance amplifier is followed by a single pole RC lowpass filter. Using an HP 3562A dynamic signal analyzer, the frequency response of the transconductance amplifier circuit with a 10 MΩ "dummy" resistor was measured and is shown in Fig. 4A. The spectral noise density was measured under the same conditions and is shown in Fig. 4B. The total noise over the bandwidth from 10 mHz to 100 Hz was computed from this data and found to be 85 pA_{rms}.

The voltage-follower amplifiers for electrophysiology measurements utilize very low noise op-amps and are preceded by back-to-back signal diodes to prevent op-amp latch-up when power is applied. Amplifier bandwidth (−3 dB) is DC to 600 kHz (Fig. 4C). Spectral noise density is shown in Fig. 4D; total noise over the bandwidth from 10 Hz to 600 kHz was calculated to be 0.14 $\mu V_{rms}/\sqrt{Hz}$ with the input shorted. The peaking observed in the noise measurements near the −3 dB frequency will have little to no effect on system performance because the electrophysiological instrument that will be connected to this output has a smaller bandwidth. Noise measurements were performed using a Rohde and Schwarz FSVR spectrum analyzer.

3. Results and discussion

3.1. Recording site characteristics

Mean impedances for 18 electrophysiology contacts (across nine devices) are provided in Table 1. Most electrodes had impedances of ~0.5 MΩ at 1 kHz. These contacts are well suited for the local field potential recordings reported below. The two contacts on a single device tend to have very similar impedances. Later fabrication batches reveal that the modal impedance is raised to approximately 1–1.5 MΩ by decreasing the contact size from 15 × 15 μm to 10 × 15 μm.

The limit of detection (LOD) and selectivity (choline to ascorbic acid ratio) of electrochemical recordings depend on variables within the fabrication process and on the enzyme coating. Electrochemical calibration results are shown in Table 2 for the choline and sentinel channels from five of the nine devices reported in Table 1. The other four devices were not coated with enzymes. Three of the five devices were then used for *in vivo* recording, their post-recording calibration values also appear in Table 2. It is clear from these data that, as would be expected, the enzyme and mPD exclusion layers deteriorate over time *in vivo*—the devices were in the tissue for approximately 6 h. We have yet to characterize the temporal profile of this decline in sensitivity and selectivity but note that all of the electrochemical data reported below come from the first 90 min *in vivo*. Re-use of these recording devices is possible with cleaning and re-coating with enzyme.

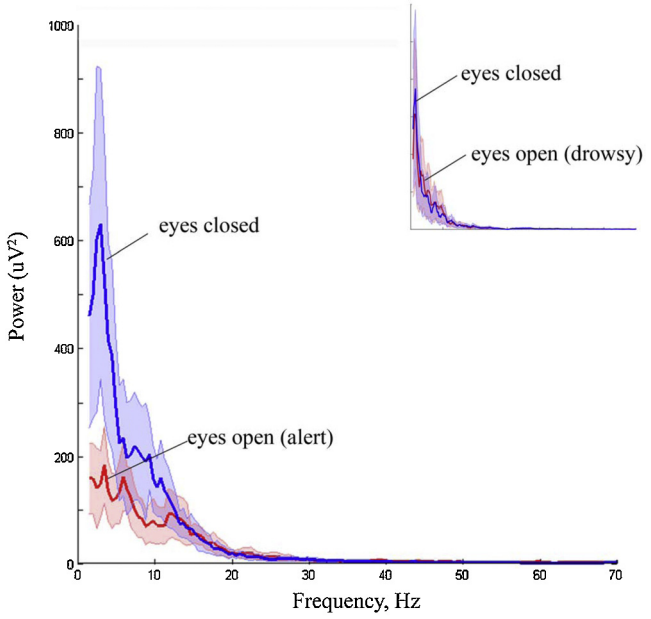

Fig. 5. Local field potential recordings in V1 across arousal states. Power spectra are plotted below 70 Hz for "awake" (red) and "drowsy" (blue) periods, behaviorally defined. An awake period was recorded when the animal had his eyes fully open for at least 2 min, a drowsy period when the eyes were closed for at least 2 min. These same behavioral criteria were used to mark "awake" and "drowsy" time periods during both electrophysiological and electrochemical recording. The data represent averages for five 2-s LFP segments taken from the first 2 min after the animal's observable behavior reached criterion. Shaded regions: SEM. Inset: There is no difference in the LFP power spectra if one compares periods with the eyes closed with periods when the eyes are open (confirmed by eye tracking) but the animal is about to go to sleep (drowsy: the 2 min prior to a "sleep" period; sleep defined as for the main figure). (For interpretation of the references to color in this figure legend, the reader is referred to the web version of this article.)

3.2. Local field potential recordings

States of arousal can be identified in the local field potential (LFP) recorded in the cortex. As an animal becomes drowsy and enters slow-wave sleep, power in the slow (<1 Hz) and delta (1–4 Hz) bands increases (Destexhe et al., 1999). Fig. 5 shows the power spectra of the recordings made with a 0.5 MΩ electrophysiology contact for one period during which the animal was classified as "awake" by observable behavior (his eyes were fully open for >4 min, red trace) and a period when he was classified as "drowsy" or asleep (eyes closed for >4 min, blue trace). This figure shows that the electrodes make excellent LFP recordings. We can also use this as a validation of the use of the "eyes open/eyes closed" dichotomy as a behavioral criterion indicative of the broad state of arousal. The power spectrum in the eyes-closed state in Fig. 5 shows strong power below 4 Hz which is characteristic of, in fact comprises a major component of the clinical definition for, the transition to slow-wave sleep (Davis et al., 2011). While it is known that transitions between having one's eyes closed *versus* open during wakefulness will change electroencephalogram (EEG) power in all frequency bands, both in a lighted room (Barry et al., 2007) and in the dark (the comparable condition for our control study: Boytsova

Table 3
In vitro device calibration.

	Baseline (nA)	Ascorbic acid (nA)	Choline 1 (nA)	Choline 2 (nA)	Choline 3 (nA)	Dopamine (nA)
Choline	−0.051	−0.059	−0.448	−0.696	−0.962	−0.937
Sentinel	−0.035	−0.041	−0.126	−0.179	−0.249	−0.240

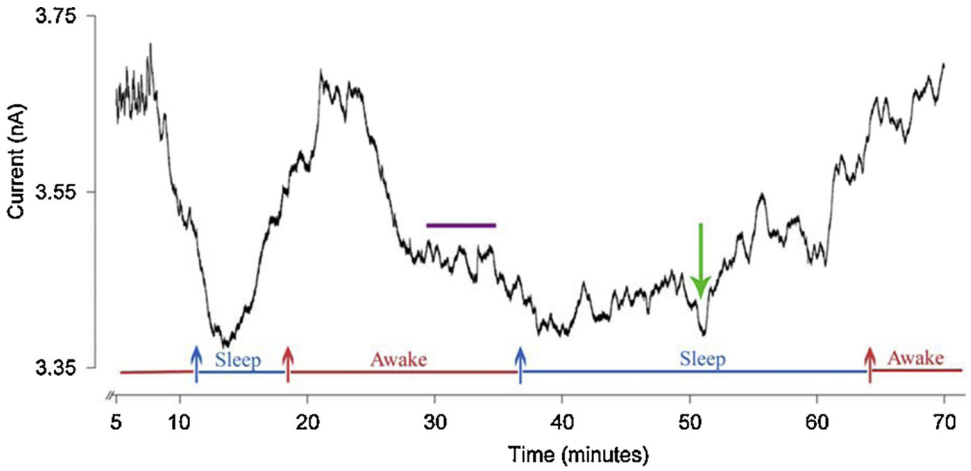

Fig. 6. Electrochemical detection of choline across arousal states in the primary visual cortex of a rhesus macaque. The current on the sentinel channel (no enzyme coating) was subtracted (point by point) from the current on the data channel (choline oxidase coating). The resulting current difference is plotted here. Recordings were made with respect to a solid AgCl pellet electrode. Red arrows indicate the points in time at which the animal reached the behavioral criterion for wakefulness (full 2 min with his eyes open). The subsequent periods of wakefulness are indicated by red bars ("awake"). Blue arrows indicate the points in time at which the criterion for sleep was reached (full 2 min with his eyes closed). The subsequent periods of sleep are indicated by blue bars ("sleep"). The magenta bar indicates a time window during which the experimenter (AD) was moving about in the recording room. The green arrow indicates a point at when the experimenter (AD) clapped and turned the room lights off and on again in an attempt to rouse the animal. (For interpretation of the references to color in this figure legend, the reader is referred to the web version of this article.)

and Danko, 2010), the changes are concentrated in higher spectral bands, particularly alpha (7–13 Hz) and beta (13–30 Hz). The spectral content of LFPs over the sleep/wake cycle mimics that observed in the EEG (Lin and Gervasoni, 2008). Having eyes open per se is not sufficient to lower delta power: if we instead calculate the LFP power spectrum in the 2 min immediately before the eyes close (when the animal has eyes open but is drowsy and approaching sleep, eyes being open confirmed by video eye tracking) and use this as our "eyes open" data, there is no difference between this and power spectrum and that obtained with the eyes closed (Fig. 5, inset: note that the inset data were gathered on a different recording day, from a different animal, to that shown in the main body of the figure). Thus the strong delta band power reflects the state of the animal, not merely the state of the eyes.

3.3. Electrochemical detection of local choline

Table 3 shows the *in vitro* calibration of the electrochemical recording sites on the device used to make the *in vivo* recordings reported here. The data channel (top row of Table 3) on this device had an excellent limit of detection (LOD) at .04 μM choline and a choline-to-ascorbic acid selectivity ratio of 64. This is the best LOD achieved in our device fabrication and preparation so far; it is attributable at least in part to excellent results in enzyme coating and mPD electropolymerization—the data below are for the second time this device was used *in vivo*. On its first use it precalibrated with a 0.65 μM LOD, an order of magnitude less sensitive and closer to the cross-device average of 0.8 μM. Thus, post fabrication variables significantly contribute to the electrochemical recording properties. This is not the case for the electrophysiology contacts. Both contacts on this device tested at 0.5 MΩ at 1 kHz every time the device was characterized—over a month of regular use and testing.

Fig. 6 shows a little over 1 h of electrochemical data recorded immediately prior to (*i.e.* on the same day, in the same animal, with the same device) as the LFP data shown in Fig. 5. It has been reported previously that acetylcholine efflux in the cortex varies with arousal (Marrosu et al., 1995; Steriade, 2004). The trace shown in Fig. 6 is the result after the current on the sentinel channel is subtracted from the current on the data channel, and so represents the signal attributable to the presence of the choline oxidase enzyme on the data channel contact. The recording has a rich temporal structure. The points in time at which the animal met the behavioral criteria for an "awake" or an "asleep" period are marked (blue and red arrows for "asleep" and "awake", respectively). It can be seen that the sleepy periods commence toward the end of a downwards slope in choline concentration in the tissue and the periods of wakefulness commence near the middle of an upwards slope in choline concentration. Thus the broad structure of the variability in choline concentration measured by this device tracks the behaviorally-defined arousal state of the animal, as expected. Some of the structure within this slow cycle of sleepiness and wakefulness appears to be related to events in the room. For example the time window indicated by the magenta bar corresponds to the experimenter (AD) moving about in the room, during which time a slow decline in choline concentration plateaus. At the point indicated by the green arrow, the experimenter (AD) clapped and turned the room lights off and on again in a (successful) attempt to wake the animal.

3.4. Summary

In combination, the recording device and UEI chassis we describe here extend our ability to observe activity within cortical circuits to enable the measurement of volume transmitted neuromodulators, opening up the possibility of a deeper understanding

of the diverse forms of state-dependent neural activity in the mammalian brain. We also extend the capacity for fast timescale recording of the concentration of extracellular molecules – previously conducted in rodents, or in short term experiments in large mammals without behavioral control – to longer-term investigations in the awake and behaving non-human primate, engaged in tasks that exert control over cognitive variables of interest.

Acknowledgements

Support for the *in vivo* recording described in this paper was generously provided by A. Nandy, J. Mitchell and K. Williams. G. Quintero, G. Gerhardt, F. Pomerleau, and P. Huettl provided valuable early training and insight into the design demands for array recording in electrochemistry. Thanks to the staff at the CalIT Nano3 facility at the University of California, San Diego for their assistance. This work was supported by National Institutes of Health grants K99 MH-93567 to AAD, R01 EY-021827 to JHR, NEI core grant for Vision Research P30 EY19005 to the Salk Institute and by the Gatsby Charitable Foundation.

References

Barry RJ, Clarke AR, Johnstone SJ, Magee CA, Rushby JA. EEG differences between eyes-closed and eyes-open resting conditions. Clin Neurophysiol 2007;118:2765–73 (official journal of the International Federation of Clinical Neurophysiology).

Bickford-Wimer P, Pang K, Rose GM, Gerhardt GA. Electrically-evoked release of norepinephrine in the rat cerebellum: an in vivo electrochemical and electrophysiological study. Brain Res 1991;558:305–11.

Boytsova YA, Danko SG. EEG differences between resting states with eyes open and closed in darkness. Hum Physiol 2010;36:367–9.

Burmeister JJ, Moxon K, Gerhardt GA. Ceramic-based multisite microelectrodes for electrochemical recordings. Anal Chem 2000;72:187–92.

Davis CJ, Clinton JM, Jewett KA, Zielinski MR, Krueger JM. Delta wave power: an independent sleep phenotype or epiphenomenon? J Clin Sleep Med 2011;7:S16–8 (JCSM: official publication of the American Academy of Sleep Medicine).

Dayan P. Twenty-five lessons from computational neuromodulation. Neuron 2012;76:240–56.

Destexhe A, Contreras D, Steriade M. Spatiotemporal analysis of local field potentials and unit discharges in cat cerebral cortex during natural wake and sleep states. J Neurosci 1999;19:4595–608 (the official journal of the Society for Neuroscience).

Hefti F, Felix D. Chronoamperometry in vivo: does it interfere with spontaneous neuronal activity in the brain? J Neurosci Methods 1983;7:151–6.

Lin SC, Gervasoni D. Defining global brain states using multielectrode field potential recordings. In: Nicolelis MAL, editor. Methods for neural ensemble recordings. Boca Raton, FL: CRC Press; 2008.

Marder E. Neuromodulation of neuronal circuits: back to the future. Neuron 2012;76:1–11.

Marrosu F, Portas C, Mascia MS, Casu MA, Fa M, Giagheddu M, et al. Microdialysis measurement of cortical and hippocampal acetylcholine release during sleep-wake cycle in freely moving cats. Brain Res 1995;671:329–32.

Parikh V, Kozak R, Martinez V, Sarter M. Prefrontal acetylcholine release controls cue detection on multiple timescales. Neuron 2007;56:141–54.

Parikh V, Pomerleau F, Huettl P, Gerhardt GA, Sarter M, Bruno JP. Rapid assessment of in vivo cholinergic transmission by amperometric detection of changes in extracellular choline levels. Eur J Neurosci 2004;20:1545–54.

Park J, Takmakov P, Wightman RM. In vivo comparison of norepinephrine and dopamine release in rat brain by simultaneous measurements with fast-scan cyclic voltammetry. J Neurochem 2011;119:932–44.

Stamford JA, Palij P, Davidson C, Jorm CM, Millar J. Simultaneous "real-time" electrochemical and electrophysiological recording in brain slices with a single carbon-fibre microelectrode. J Neurosci Methods 1993;50:279–90.

Steriade M. Acetylcholine systems and rhythmic activities during the waking—sleep cycle. Prog Brain Res 2004;145:179–96.

Takmakov P, McKinney CJ, Carelli RM, Wightman RM. Instrumentation for fast-scan cyclic voltammetry combined with electrophysiology for behavioral experiments in freely moving animals. Rev Sci Instrum 2011;82:074302.

Vizi ES, Kiss JP, Lendvai B. Nonsynaptic communication in the central nervous system. Neurochem Int 2004;45:443–51.

Zhang H, Lin SC, Nicolelis MA. Acquiring local field potential information from amperometric neurochemical recordings. J Neurosci Methods 2009;179:191–200.